Twin spin model of surface phase transitions in O/W(110)

Magdalena A. Załuska-Kotur
Institute of Physics Polish Academy of Science & College of Science, Aleja Lotnikow 32/46, 02-668 Warsaw, Poland

Stanisław Krukowski
High Pressure Research Center Polish Academy of Sciences, Sokołowska 29/37, 01-142 Warsaw, Poland

Zbigniew Romanowski
Department of Physics, Warsaw Technical University, Koszykowa 75, 00-672 Warsaw, Poland

Łukasz A. Turski
Center for Theoretical Physics Polish Academy of Sciences & College of Science; Aleja Lotnikow 32/46, 02-668 Warsaw, Poland
(Received 12 February 2001; revised manuscript received 17 July 2001; published 26 December 2001)

A model describing surface phase transitions in an O/W(110) system is proposed. The model is based on the hourglass structure of adsorption sites of oxygen on tungsten surface. The hourglass structure of the site in the O/W(110) system has been confirmed by quantum mechanical density functional theory (DFT) calculations. The results of DFT calculations indicate that the saddle point at the center has the energy 0.2 eV higher than two symmetric minima. An essential ingredient of the model is the assumption that the interaction of O atom with the other O atom, located in nn site, lifts the degeneracy of the two energy minima, converting the hourglass structure of the adsorption site to a single state site. The O/W(110) adsorption model can be projected onto a system consisting of double spins distributed on a two-dimensional square lattice. The properly chosen two-body interactions in the square lattice double-spin system are capable of recovering all phase transitions that are observed in the O/W(110) system. Due to well known mapping between spin and the lattice gas systems, the proposed model can be used to describe multidomain structure in the O/W(110) system.

DOI: 10.1103/PhysRevB.65.045404 PACS number(s): 68.35.Fx, 66.30.−h, 05.50.+q

I. INTRODUCTION

The analysis of the physical properties of gases adsorbed on solid surfaces continue to be an important area of both theoretical and experimental research. These systems are attractive to the theoreticians due to the fact, that wide variety of the adsorbate two-dimensional (2D) lattices and possible interadsorbate interactions allows one to test various assumptions built into plethora of available phase transformation models, and compare the results with experimental available data.[1–28] Oxygen on tungsten (110) surface is one of the most studied model adsorption systems. The existence of different, coverage dependent, phases allows one to study various phenomena: phase structure and phase coexistence, condensation, kinetics of ordering as well as equilibrium and far from equilibrium diffusion processes.[1–28]

The lattice-gas model with properly chosen interaction constants is believed to describe properly phase transitions existing in the O/W(110) system. There are several suggestions for the set of interaction constants.[8–14] The basic models that have been proposed in the literature to describe O/W(110) are constructed using square lattice gas with competing nearest-neighbor and next-nearest-neighbor interactions.[5–16] The absence of the particle-hole symmetry in the experimentally observed phase diagram suggests introduction of at least three-body interactions to the model. The strength of these three-body interactions has to be of the same order as that of the two-body forces.[5–16] This implies that three-body interactions are of relevance for the whole phase diagram, not only its low-density part. In this paper, however, we show that the asymmetry of the phase diagram can be reproduced when instead of three-body interactions, the simple lattice gas model is expanded by an additional particle state. The existence of various states of the same adsorbed particle can be explained by the change of the energetic structure of the adsorption site resulting from the interaction with the oxygen atom located in nearest neighbor site.

The adsorption site at W(110) surface has hourglass shape[1,3] suggesting that the center and the symmetric twin triply coordinated positions are possible candidates for the location of O adatom. It follows from the existence of site-exchange domain superstructures, observed by use of low energy electron diffraction[14,15,29] and scanning tunneling microscopy[16] that oxygen adatom occupies one of the two ends of this space, i.e., triply coordinated locations. These conclusions have been confirmed by the detailed analysis of high resolution core-level photoelectron spectroscopy (PS) measurements.[29,30] It has been shown that sequence of quantum states denoted as O1, O2, and O3, corresponds to the location of single O atom in triple coordinated site creating on W-O quantum state.[29] The O2 and O3 states are created due to localization of two and three O atoms close to W atom for higher coverages. The O2 state corresponds to $p(2\times1)$ structure whereas O3 corresponds to $p(2\times2)$ and (1×1) structures, observed by the low-energy electron diffraction (LEED) pattern.[29] In case of the central position the sequence of the energies should be different, reflecting the existence of two different pairs of W-O neighbors. The absence of such observation strongly favors the model of twin sym-

metric positions. Those two positions can, in principle, have the same energy.

The energy landscape studies above were supplemented by kinetic measurements.[29] These results show that O atoms are immobile at 360 K and have low mobility at 598 K. The energy barrier for O diffusion at 0.3 ML coverage is about 0.61 eV.[3,5–7] The barrier depends on coverage, for coverage of 0.56 ML the barrier increases to 0.96 eV.[29]

The double-well model has been used in Refs. 15 and 16 in order to describe those physical properties of O/W(110), in which degeneracy of ordered state plays an important role. We draw on this model here in construction of a novel lattice gas model, analysis of which shows existence of experimentally observed phases. Contrary to previous works no three body interactions are needed to describe full phase diagram. The price we pay is the abandoning of the simplicity of two state (0–1) lattice gas, which is replaced by that with three different states. Such three-state model can be easily expressed in terms of two Ising spins attached to each lattice site.[31]

To determine the energy of the adsorbed single O atom on W(110) surface we have performed quantum mechanical calculations in density functional theory (DFT) formulation using cluster model of W(110) surface. The model and the results of the DFT calculations are presented in Sec. II. In Sec. III the model for O/W(110) is introduced including discussion of the choice of the interaction constants and interaction dependent site structure. This is followed by the analysis of the equilibrium lattice gas properties by means of the Monte Carlo simulations, and subsequently by the mean field analysis and the discussion of the properties of the system, including the existence of ordered phases. These results are summarized in the last section of the paper.

II. QUANTUM MECHANICAL DFT CALCULATIONS: ATOMIC CLUSTER APPROACH

In order to determine the most favorable lattice sites for adsorption of oxygen on W(110) surface we have used the finite cluster model for representation of the infinite surface. It is well known that the cluster models suffer of the significant numerical errors and poor size convergence with respect to the absolute energy values and bonding energies.[32–35] Relative energies are, however, obtained with much smaller errors; therefore one can determine more precisely the most favorable lattice sites and the energy barriers.

Quantum mechanical (QM) many body Schrödinger equation was solved using density functional theory formalism, based on Hohenberg-Kohn[36] and Kohn-Sham theorems.[37] The QM equations were solved using commercial DMOL package distributed by MSI Inc.[38] The DFT method replaces multidimensional linear equation by nonlinear equation for electron density. This transformation requires expression of all terms in Hamiltonian in function of the electron density. This reduction is exact for all terms in Hamiltonian with exception of the exchange and correlation terms. The latter terms were expressed in Becke approximation for the exchange energy[39] and the Lee-Yang-Parr (LYP) approximation for correlation energy.[40] In numerical solution procedure,

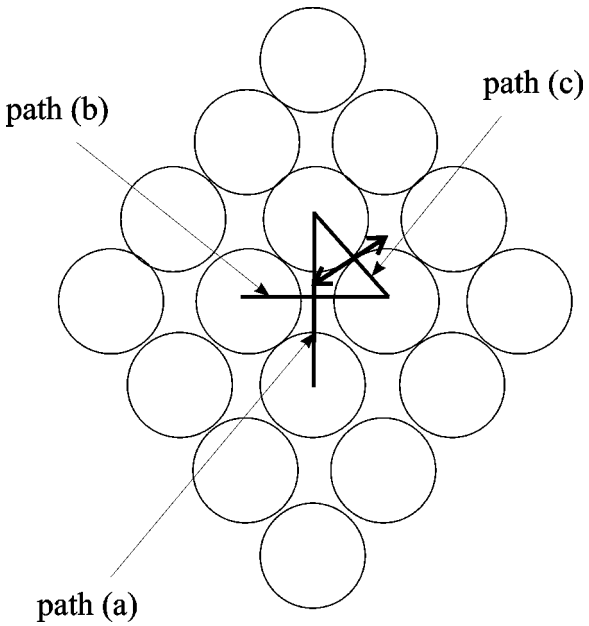

FIG. 1. The geometry of the W cluster used for QM calculations: circles corresponds to W atoms; the lines denote path used for determination of the energy barriers; double arrows indicate preferential path for the jumps between the minimum energy locations.

employed in DMOL package,[38] the continuous electron density distribution is represented on finite number of the lattice points. In general higher number of the grid points allows for better representation of the density distribution, on the other hand, it puts higher requirements for the available computer memory and the CPU speed. Therefore careful choice of the computational grid is crucial for proper representation of the electron density. The nonlinear matrix equations, with matrix elements corresponding to the electron density at the grid points, have been solved using iterative procedure in Newton-Raphson scheme. During iterations, the W atoms positions were relaxed to the minimum energy locations. The iteration/relaxation procedure has been terminated after the two following conditions were fulfilled simultaneously: the electron density change was not higher than 10^{-4} eV and energy change was not higher than 2×10^{-5} eV. In most of the calculations up to 20 iterations were necessary to reach convergence.

The quantum mechanical calculations were performed using total or partial freeze of the W atomic cores. The total freeze of the atomic cores led to the divergence of the Newton-Raphson iteration procedure. Only when the external atomic shell is considered explicitly in the DFT solution, the iteration procedure converged. This indicates that the electron belonging to the cores of W atoms play a very important role in bonding of tungsten crystals. The cluster model, which we used as a representation of infinite W(110) surface consisted only of one atomic layer with lattice symmetry corresponding to W(110) surface.

The total number of atoms was 16. The arrangement of the tungsten atoms, the possible lattice sites for oxygen adsorbed on the surface and the transition paths between the sites are shown in Fig. 1. The calculation begins with the

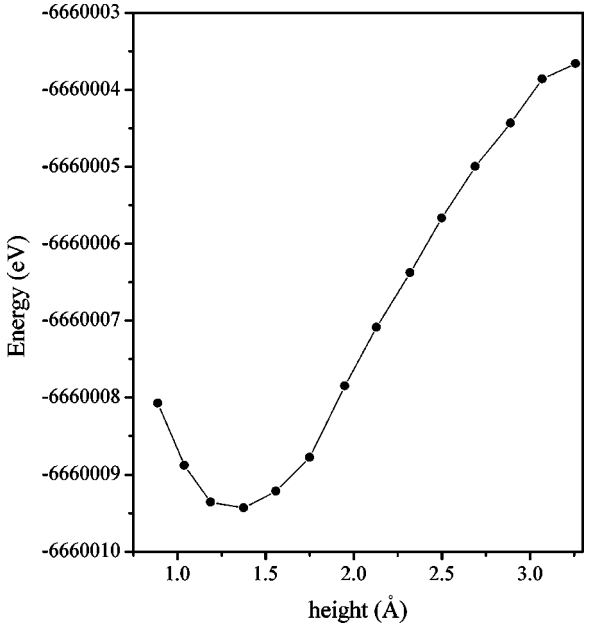

FIG. 2. Total energy of the cluster vs O-W distance, calculated by QM DFT procedure. The oxygen atom is located above the center of the cluster. The points represent the calculated values, the line is inserted to guide the eye.

cluster where tungsten atoms were located in the lattice sites, corresponding to tungsten lattice constant equal to 3.14 Å. Then the W atoms were relaxed toward minimal energy position using adiabatic approximation for quantum mechanical calculations. The relaxation procedure preserved the symmetry of the cluster and kept all the atoms in one plane. The relaxations of the W atomic positions led to the finite lattice of about 3.0 Å lattice constant. The difference is caused by finite size of the use of one layer only and finite size of the cluster.

The total energy of the system consisting of single O atom and W cluster has been calculated by localizing the O atom. In order to find the minimum, the total energy of the system has been calculated using the intervals distance between the O atom and the tungsten plane equal to 0.2 Å. The example of such energy vs W-O distance curve, calculated for the oxygen located above the center of the W cluster, has been presented in Fig. 2. The energy curve shows that O atom is strongly attracted by the W cluster. The minimum energy point lies at the distance about 1.3 Å from the W surface and corresponds to the energy about 6 eV below the energy that has oxygen atom far away from the surface. This energy counted twice for O atoms gives 12 eV, which is way above the O_2 dissociation energy equal to 5.08 eV. That indicates that O_2 adsorption on W(110) surface has no energy barrier, which is similar to adsorption of O_2 on Al surface.[35] This is in agreement with the assumptions made by Ynzunza *et al.*[29] that adsorption of O_2 on W(110) surface leads to immediate dissociation of the oxygen molecule.

We were looking for the lowest energy positions of the oxygen adatoms and for the optimal path for the adatom site to site jump. The first result is the basis of the static model of the oxygen adatom layer. The second result determines the

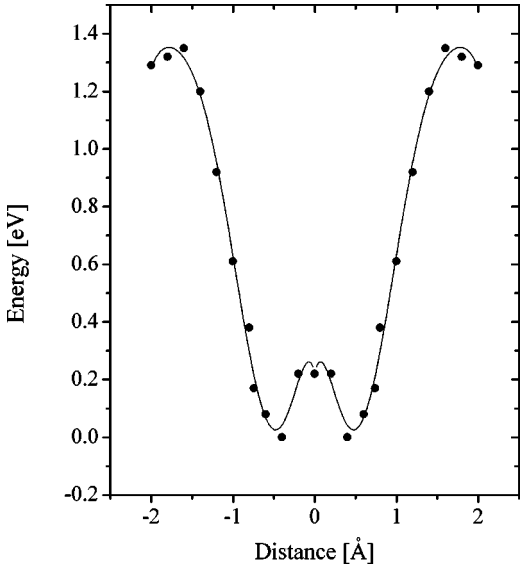

FIG. 3. The results for the path (a). The energy of the O atom as a function of its position along longer diagonal of the rhombus: points are the calculated values of the energy and line is the polynomial fit.

barriers for jump and is a necessary step for the calculations of the dynamical properties of the O/W(110) system, that will be the subject of our next work. Both energies can be obtained by analyzing the adiabatic total energies. The total energies have been calculated for three different paths, along the W(110) surface. These paths, labeled (a), (b), and (c), correspond to the long and short diagonal and the edge of the rhombus. The energy of the system was obtained for the points separated by 0.2 Å. The results are presented in Figs. 3, 4, and 5 for paths (a), (b), and (c), respectively. In Figs. 3–5, the points correspond to the calculated values, the lines

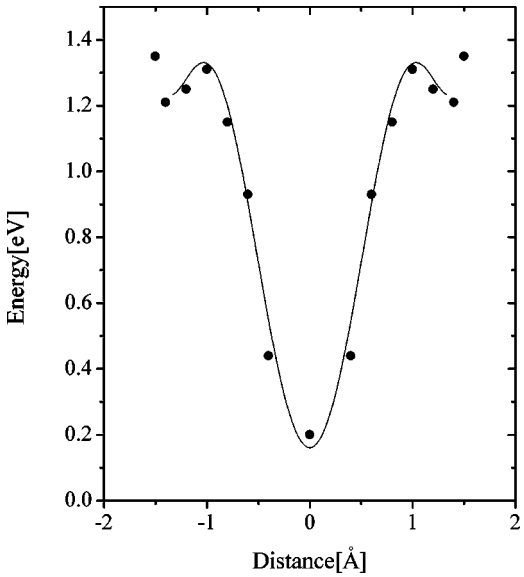

FIG. 4. The results for the path (b). The energy of the O atom as a function of its position along shorter diagonal of the rhombus: points are the calculated values of the energy and line is the polynomial fit.

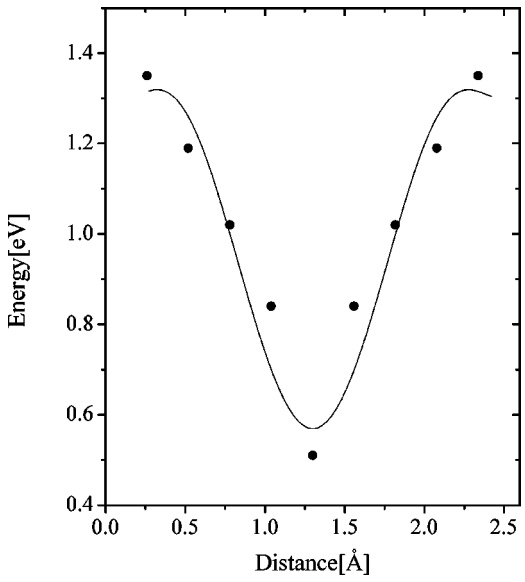

FIG. 5. The results for the path (c). The energy of the O atom as a function of its position along the side of the rhombus: points are the calculated values and line shows polynomial fit.

result from the polynomial fit to the calculated data.

The energy calculated for the path (a), i.e., along the longer diagonal of the rhombus, presented in Fig. 3, has two deepest minima corresponding to the localization of the O atom symmetrically, at the distance about 0.45 Å from the center of the rhombus. This position is in quite good agreement with the results of LEED measurements of Ynzunza *et al.*[29] For O1 structure they obtained the shift $1=1.67$ Å. In our case we have to subtract from center-W distance, equal to 2.12 Å the calculated value 0.45 Å, which gives exactly the same value. We feel that so good agreement is a little bit fortuitous.

At the center of the rhombus, the energy is about 0.2 eV higher. There is a possibility of a very shallow minimum at the center, of the depth of about 0.02 to 0.03 eV, which is below accuracy of our calculations. Again the height of the central barrier of 0.2 eV is in agreement with the temperature dependent PS measurements of Ynzunza *et al.*[29] They observed that at 598 K the O atom is still located at triply coordinated site. The height of the barrier equal to 0.2 eV is sufficient to explain the observed effect. For larger distances from the center of the rhombus, the energy steeply rises up to about 1.4 eV. The energy is so high that the direct transition of the O atom along this path can be neglected in analysis of the diffusion processes.

There is also no contradiction between the height of the central energy barrier and the measurements of the anisotropy diffusion coefficient.[17] Diffusive behavior of particles in two-well adsorption site structure has been discussed in Ref. 41. It has been shown that the diffusion anisotropy is given by[41]

$$\frac{D_{yy}}{D_{xx}}=\frac{r}{r+2}\left[\frac{b}{a}\right]^2. \tag{1}$$

It is determined by the branching ratio $r=M/I$, where M is rate for intersite jump and I is rate for jumps out of the site, a and b denote the dimensions of the underlying unit cell. $(b/a)^2=2$ for W(110). The branching ratio $r \cong \exp(0.3\,\mathrm{eV/kT})$, and changes from $r=60$ to 10^5 within the range of observed temperatures. That is in agreement with experimental measurements of the diffusion anisotropy for O/W(110) being close to 2.[17]

The energy curve corresponding to path (b), i.e., along the shorter diagonal of the rhombus, is presented in Fig. 4. The energy has the minimum at the center of the rhombus and increases quickly for the distances up to 1 Å. At the localization on top over W atom, very high maximum exists. The height of this maximum is roughly the same as for the previous path, which again leads to the conclusion that this path can be neglected in the simulation of the diffusion processes.

The last energy curve corresponds to path (c), i.e., the path along the side of the rhombus, is shown in Fig. 5. The curve has two maxima corresponding to the positions of the O atom on top of W atoms. The energy has the minimum at the center, roughly 0.8 eV below the energy level of the maxima. From these results, i.e., comparing the energy difference for path (a) which was 1.3 eV and for the path (b) i.e., 0.8 eV one can conclude that the energy of the barrier for the transition across the line connecting two W atoms is about 0.5 eV. This is in basic agreement with the diffusion barrier equal to 0.6 eV, derived from the temperature dependence of the oxygen diffusion on the W(110) surface.[5–7]

The QM calculations sketched above allows us to draw a set of conclusions as to the possible O atom migration dynamics on the W(110) surface

(i) The only relevant possible path of the jumps of the O atoms is that across the side of the rhombus, as indicated by the double arrow in Fig. 1.

(ii) The absolute minimum of the energy (adsorption site) is shifted by about 0.45 Å from the center of the rhombus.

(iii) The difference of the energy between the absolute minimum and the center of the rhombus is relatively small, about 0.2 eV.

The interactions with the closest near-neighbor (NN)O adatoms can displace the O atoms from these locations, leading to the disappearance of the energy minima far, and localization of O atom close to the center of the rhombus.

III. TWO SPIN LATTICE MODEL AS A DESCRIPTION OF SINGLE ADLAYER

Consider now a single O/W(110) adlayer. According to the experimental results[15–23] it has two basic ordered phases and several coexistence regions. There is transition from disordered to (2×1) striped phase at the low density part of the phase diagram. This transformation is believed to be of second order at higher temperatures and it becomes the first order one with wide coexistence region when the system is cooled. Such behavior can be explained when one assumes two types of adparticle interactions, both of similar strength: attractive between nearest neighbors and repulsive between next-neighboring sites. The presence of second neighbor interactions causes that this model is not related to any known

analytically solvable systems. Numerical analysis shows that it reproduces phase changes very well up to density 0.5.[5,8] Unfortunately higher adatom concentrations lead to a new phase (2×2) which has no reverse copy at low densities. Such phase can be modeled in existing lattice gas system by adding three particle interactions, which breaks particle-hole symmetry (present in every lattice gas model with two-body interactions). Three-body interactions, that have to be added to the Hamiltonian to reproduce measured static properties of oxygen layer, are strongly repulsive. Their strength is of the same order as two previously introduced interactions.[11–13] These interactions, and shape of resulting phase diagram depend on the details of the model—for example, on the choice of sites connected by three body interactions.[11–13] Since experimental data are very incomplete, it is very hard to conclude which of these *ad hoc* constructions is close to the reality. The physical consequence of the lack of the particle-hole symmetry is the existence of the surface stress. We have seen in our DFT calculations that the surface of tungsten is very soft. The oxygen atom drags tungsten atoms closer toward its position, and because of this it has indirect, beside direct influence onto other adatoms. Such indirect interaction can have effectively three-body character.

The above interpretation is, however, not the only one possible. The same physics can be explained assuming that the adatom can be in one of three possible states chosen in agreement with all direct and indirect interactions with the host lattice and with neighboring particles. Assuming that we can use a very simple pattern of adatom interactions, that leads, in a robust way, to the proper sequence of the adsorbate phase transitions. The other advantage of such a model is the existence of various domains which correspond to those observed experimentally in Refs. 13 and 14.

The construction of our new model is as follows. The oxygen atom can be placed in one of the three possible locations. Two of them are having the same low energy and correspond to positions at opposite ends of hourglass space between tungsten atoms. These two closely located energy minimums A and B are separated by small energy barrier. Third possible location C is at the saddle point between these minimums, as shown in Fig. 1. An oxygen adatom, located at this place has an additional energy V equal to the barrier for jump between two triply coordinated minimums A and B. Hence the position C is not energetically favored for a single separated adatom, far from the other neighbors (low-density situation). When the density increases the interactions with other atoms can change that situation, and result in making that very position energetically favorable.

Now, assuming that the double occupancy is forbidden we see that the adatom occupying one adsorption site can be at one of three states A,B,C, or that the site is empty 0. Therefore there are four possible states available to the adatom at a given lattice site. These four states can be represented by two (fictitious) spins $(s,\sigma)=(\pm1,\pm1)$. the spin arrangements corresponding to our four states are $(1,-1)$ describes state A, $(-1,1)$ describes state B, $(1,1)$ describes state C, and $(-1,-1)$ denotes the empty site.

We found it more convenient to introduce yet another variable, the product of $u=s\sigma$. Its value $u=\pm1$, discriminates between both minima A,B, for which $u=-1$, and other two states C, 0 with $u=1$. Variables u and s allow us to write the system Hamiltonian as

$$H=\frac{1}{2}J\sum_{(ij)}u_is_is_j+\frac{1}{8}J_2\sum_{\mathrm{NNN}}u_iu_j-\frac{1}{4}J'\sum_{3n}(u_iu_j+1)s_is_j+\frac{1}{4}[V-\mu+8(J-J')]\sum_i(u_i+1)s_i+\frac{1}{4}(V+\mu-4J_2)\sum_i u_i-E_0, \tag{2}$$

where (ij) means summing over i and j being nearest neighbors, NNN means summing over all next-nearest neighbors, $3n$ over third-neighbor pairs, and μ is chemical potential. Note that pair (i,j) and (j,i) are counted as independent. The last term $E_0=-0.25V+0.75\mu-2J+2J'-0.5J_2$ is the energy of unoccupied site. First term in Eq. (2) describes state-dependent interactions between nearest neighbors, it can be rewritten as

$$\frac{1}{2}J\sum_{(ij)}u_is_is_j=\frac{1}{4}J\sum_{(ij)}[(1+u_i)(1+u_j)s_is_j-(1-u_i)(1-u_j)s_is_j], \tag{3}$$

where it is easily seen that it describes repulsion between adatoms in C state, attraction between AA and BB, and repulsion between A and B. The second term of Eq. (2) means that variable u_i has tendency to order antiferromagnetically for every second site. The third term of the Hamiltonian causes those particles in the next nearest neighboring rows do interact, and prefer to occupy the same state A or B. Nonzero potential V means that state configuration $u_i=s_i=1$ representing state C has higher local energy.

Equation (2) can be rewritten in terms of density variables using relations

$$n_i^A=\tfrac{1}{4}(1-u_i)(1+s_i), \tag{4}$$

$$n_i^B=\tfrac{1}{4}(1-u_i)(1-s_i), \tag{5}$$

$$n_i^C=\tfrac{1}{4}(1+u_i)(1+s_i), \tag{6}$$

where n_i^A, n_i^B, $n_i^C=0,1$ are occupied at A, B, and C states. Several simple relations such as Eq. (3), $n_i^A-n_i^B=(1-u_i)s_i/2$, and $n_i^A+n_i^B=(1-u_i)/2$ can be helpful in deriving the following form of the Hamiltonian:

$$H=-J\sum_{(ij)}(n_i^A-n_i^B)(n_j^A-n_j^B)+J_2\sum_{\mathrm{NNN}}(n_i^A+n_i^B)(n_j^A+n_j^B)+4J\sum_{(ij)}n_i^Cn_j^C-2J'\sum_{3n}n_i^Cn_j^C-J'\sum_{3n}(n_i^A+n_i^B)\times(n_j^A+n_j^B)+V\sum_i n_i^C-\mu\sum_i(n_i^A+n_i^B+n_i^C). \tag{7}$$

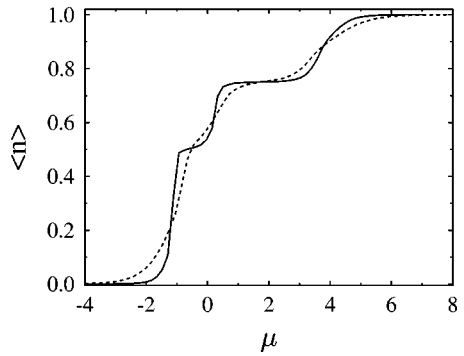

FIG. 6. Mean density n vs chemical potential for $k_BT=0.55J$, $k_BT=0.35J$, and system size 20×20

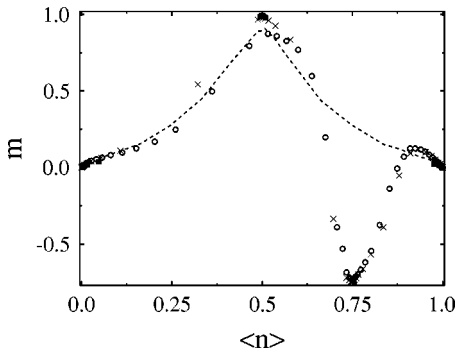

FIG. 7. The density dependence of the order parameter m for our model [at $k_BT=0.55J$ (circles) and $k_BT=0.35J$ (crosses)] compare with that for a simple lattice gas model (dashes for $k_BT=0.55J$, and squares for $k_BT=0.35J$). Curves have been calculated for 20×20 samples.

We can go also one step further and use just one variable $n_i=n_i^A+n_i^B+n_i^C$. For low densities our Hamiltonian can then be written in terms of n. This Hamiltonian contains then three-body interactions and improving its validity for higher densities requires addition of even higher multiparticle interactions. In that fashion one can establish connections with the many-body Hamiltonians discussed in Ref. 31.

IV. EQUILIBRIUM SOLUTIONS

To analyze the details of our model we choose the following interaction constants $J_2=1.5J$, $J'=-0.1J$, and $V=J$ ($J\simeq0.1$ eV). The values are chosen in such a way as to reproduce the diluted lattice gas model properties with first neighbors interaction strength $J_0=-1$, second neighbors $J_0'=0.806$ and third neighbors $J_0''=-0.203$.[8] The gross features of the phase diagram, types of phases that are present can be seen from the plot of mean density $\langle n\rangle=\Sigma_i n_i/N$ vs chemical potential μ. We show in Fig. 6 the dependence of mean density on chemical potential at two temperatures $k_BT=0.55J$ and $k_BT=0.35J$. All these curves have been calculated using Monte Carlo simulations with periodic boundary conditions. Transition to (2×1) phase is of the second order at higher temperatures and of the first order at lower temperatures. For higher densities the system undergoes transition to (2×2) squared phase. It seems that transition from (2×1) to (2×2) phase is also of second order for higher and of first order for lower temperatures. Phase diagram for densities higher than $\frac{1}{2}$ is dominated by squared (2×2) squared structure, and coexistence regions of (2×1) and (2×2) and (2×2) and (1×1) structures. We can see that there are generally two ordered phases: (2×1) striped and (2×2) squared. Lines in stripped phase consist of particles in the A or B state only. Squared phase is built by A- or B-type lines and C-type particles added in rows between occupied lines. The mechanism of creation of squared phase follows from the relation between the coupling constants at various states. Repulsion between the A particle and its next-nearest neighbor in the A state is so large, that one of that adatoms is pushed up into the C state, especially when there are more than one next neighbors. State C has higher energy equal to V for separate particle, however its interaction energy is lower. Adatom at state C repels its nearest neighbor that is in state C, and this is the mechanism of creation of (2×2) state.

Analysis of energy differences for various ordering shows that at temperature close to 0 phase transitions are as follows: first from low-density disorder to (2×1) at $\mu_1=-J-2J'$, second to (2×2) at $\mu_2=V-2J'$, and third to dense (1×1) phase at lower value of two $\mu_3=4J_2-2J-2J'$ or $\mu_3'=V+8J-8J'$. We can see in Fig. 6, that for $k_BT=0.35J$ transition points are not far from those calculated at $T=0$.

To calculate order parameter for both ordered phases (2×1) and (2×2) we divide the lattice into four sublattices. Comparison of density in four sublattices allows us to tell the difference between striped and squared phases. In Fig. 7 we have plotted order parameter calculated as sum of absolute values of differences between sublattice mean densities $\langle n_\alpha\rangle=4(\Sigma_{i\in\text{sub}}n_i)/N$ and global mean density $\Delta n_\alpha=\langle n_\alpha\rangle-\langle n\rangle$, all multiplied by signs of these differences:

$$m=\frac{1}{2}\prod_{\alpha=1}^{4}\frac{(\Delta n_\alpha)}{|(\Delta n_\alpha)|}\sum_{\alpha}^{4}|(\Delta n_\alpha)|. \tag{8}$$

The defined above order parameter m equals 1 for an ideal ordering of stripped phase, and $m=-\frac{3}{4}$ for an ideal squared phase. In Fig. 7 we compare this order parameter m for our model, with that for a simple $0-1$ lattice gas with corresponding interaction constants. We can see that up to the mean density $n=\frac{1}{2}$ plots for both models are quite close to each other. The difference shows up at higher densities, where squared phase emerges.

The ordering of the surface phase can be studied by use of low-energy electron diffraction (LEED).[19–23] The intensity of LEED diffraction pattern depends on the square of the order parameter $m'=\frac{1}{2}(\langle n_1\rangle+\langle n_2\rangle-\langle n_3\rangle-\langle n_4\rangle)$. The sequence of $\pm$ signs in this order parameter definition is related to the orientation of the surface. There are many experimental data for temperature dependence of the LEED intensity O/W system.[19–23] The study of the (2×1) structure at perfect ordering $n=0.5$ density has been even used to find critical exponents of the transition.[23] We show in Fig. 8 the temperature dependence of the order parameter m' for mean density

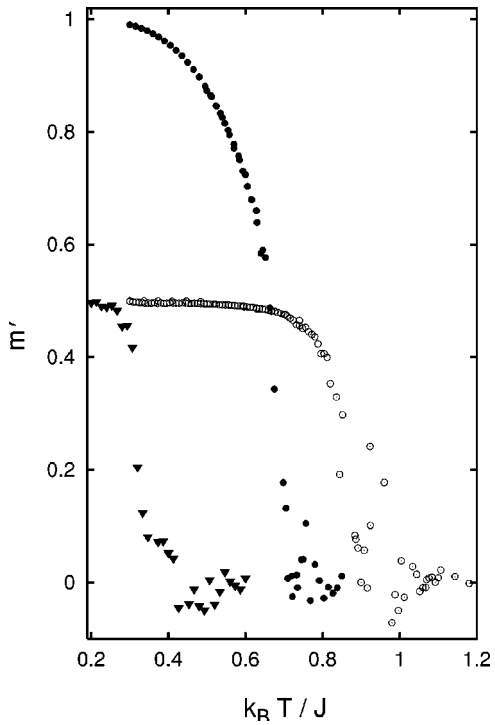

FIG. 8. Order parameter m' as a function of temperature, for fixed mean density of the system. Full circles are plotted for density $n=0.5$, open circles for $n=0.75$, and triangles for $n=0.25$. System size is 50×50.

$n=0.25$, 0.5, and 0.75. It can be seen that transition temperatures as well as the overall shape of curves agrees with experimental data. More extensive calculations are needed to obtain critical exponents. Moreover even if the phase diagram topology is stable under small changes of model parameters, critical exponents can be more sensible.[12] The angle distribution of LEED intensity reflects distribution of island size.[15,21] Again island size distribution within the presented here model needs much more precise numerical study. The model should be interesting for the study of ordering dynamics, as it gives the degeneracy of ordered phase (2×1) equal to 8, and not 4 as lattice gas models. On the basis of our simulations we can only say that the domains that are formed have no tendency to elongate in one or another direction.[8]

We have analyzed our model numerically for one particularly chosen set of its parameters. We have checked, however, that this model is quite stable, and the main features of the phase diagram are retained as long as $V<4J_2-2J$. When this condition is not fulfilled the model exhibits only one transition, namely, the (2×1) phase. When the value of the potential V is low, the (2×1) phase disappears and the only ordered dense phase is the (2×2). When in addition J and J' are of comparable strength two (2×2) phases, rare and dense, appear in the phase diagram. Finally, when the field that in Eq. (2) is coupled to variables $\Sigma_i(1+u_i)s_i$ is changed, and is given by $h=1/4(-\mu-8J-8J')$, we have model with one rare (2×2) phase only. In Fig. 9 we show examples of above described above realizations of our model. As double well structure of the adsorption site with

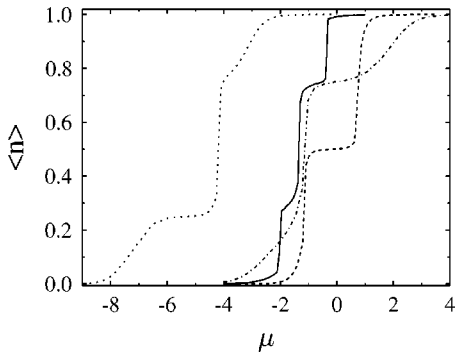

FIG. 9. $\langle m\rangle$ plotted versus μ for different realizations of our model. From left to right (a) single ordered (2×2) rare phase. Data for $V=0$ and $h_1=1/4(-\mu-4J-4J')$ at $k_BT=0.35J$ shown as the dotted line. (b) Two ordered phases, rare and dense (2×2), both for $V=0$, $J=0.27J_2$, $J'=0.33J_2$, at $k_BT=0.33J_2$ shown as the full line. (c) Same but for $V=-2J$; at $k_BT=0.35J$; shown as the dot-dashed line. (d) (2×1) phase for $V=3J$, $J_2=J$ and $k_BT=0.35J$ shown as the dashed line.

exclusion principle of double occupancy, can be found in other than O/W(110) systems, i.e., H/W(110) the model can be adapted to a description of such system. As it can be seen in Fig. 9 different phase diagrams can be realized by changing our model parameters.

V. MEAN FIELD ANALYSIS

In this section we show the mean field analysis of our model resulting with a qualitative description of the system properties. We found it convenient to write the mean field equations for the variables (in obvious notation following Sec. II):

$$\langle s^\alpha\rangle=\frac{4}{N}\sum_{i\in\alpha}s_i;\langle\sigma^\alpha\rangle=\frac{4}{N}\sum_{i\in\alpha}\sigma_i;\langle u^\alpha\rangle=\frac{4}{N}\sum_{i\in\alpha}u_i. \quad (9)$$

In order to describe symmetry of all phases we divide lattice into four sublattices numbered by $\alpha=1,2,3,4$. Mean field equations can be derived using relation

$$\langle s^\alpha\rangle=\frac{\Sigma_{\{s_i,u_i\}}s_i\exp[-\beta H(s_i,u_i\langle s^\alpha\rangle,\langle\sigma^\alpha\rangle,\langle u^\alpha\rangle)]}{\Sigma_{\{s_i,u_i\}}\exp[-\beta H(s_i,u_i\langle s^\alpha\rangle,\langle\sigma^\alpha\rangle,\langle u^\alpha\rangle)]}, \quad (10)$$

where in the Hamiltonian H (2) all spins but s_i and u_i are replaced by their mean values at corresponding sublattice. Equations for $\langle\sigma^\alpha\rangle$ and $\langle u^\alpha\rangle$ are analogous. Note that even if $\sigma_i=u_is_i$ at each site, their average values are independent, because of the correlations existing in the system. Therefore we have twelve mean field variables for which we can write the following set of equations:

$$\langle u^\alpha\rangle=\frac{X+Y-Z-V}{X+Y+Z+V},$$

$$\langle s^\alpha\rangle=\frac{X-Y-Z+V}{X+Y+Z+V},$$

$$\langle \sigma^{\alpha} \rangle = \frac{X - Y + Z - V}{X + Y + Z + V}, \tag{11}$$

where

$$X = \exp(\beta\xi + \beta\kappa + \beta\eta),$$

$$Y = \exp(-\beta\xi - \beta\kappa + \beta\eta),$$

$$Z = \exp(\beta\xi - \beta\kappa - \beta\eta),$$

$$V = \exp(-\beta\xi + \beta\kappa - \beta\eta) \tag{12}$$

and

$$\xi = -\frac{J}{2}(\langle s \rangle^{\alpha 2} + \langle s \rangle^{\alpha 4}) + J' \langle \sigma \rangle^{\alpha} - \frac{1}{4}(V - \mu + 8J - 8J'),$$

$$\kappa = -\frac{J}{2}(\langle \sigma \rangle^{\alpha 2} + \langle \sigma \rangle^{\alpha 4}) + J' \langle s \rangle^{\alpha} - \frac{1}{4}(V - \mu + 8J - 8J'),$$

$$\eta = -J_2 \langle u \rangle^{\alpha 3} - \tfrac{1}{4}(V + \mu - 4J_2). \tag{13}$$

In all these formulas superscript $\alpha 2$ means sublattice of neighboring sites in the x direction, $\alpha 4$ in the y direction, and $\alpha 3$ means the sublattice of sites in diagonal direction from α. At high temperatures we can assume that variable $\langle u \rangle$ is the one that spontaneously orders, whereas the others are disordered. When additionally we assume that $\Sigma_{\alpha}(\langle s \rangle^{\alpha} + \langle \sigma \rangle^{\alpha}) = \Sigma_{\alpha} \langle u \rangle^{\alpha} = 0$, which corresponds to mean density equal to 0.75 we can reduce Eqs. (11) to

$$\langle u \rangle^{\alpha} = \tanh(-\beta J_2 \langle u \rangle^{\alpha 3} - \Delta\mu), \tag{14}$$

where $\Delta\mu = \mu - \mu_0$ and μ_0 fulfills the following condition:

$$\cosh(\beta\xi + \beta\kappa) = \exp(-\mu_0/2)\cosh(\beta\xi - \beta\kappa). \tag{15}$$

The variable $\langle u \rangle$ behaves as order parameter of simple Ising antiferromagnetic system, and it couples to $\Delta\mu$ as in an antiferromagnet subject to external field, hence the second order transition should be expected at high temperatures. When temperature becomes lower we have

$$\langle s \rangle^{\alpha} = \langle u \rangle^{\alpha} \tanh[-\beta J(\langle s \rangle^{\alpha 2} + \langle s \rangle^{\alpha 4})], \tag{16}$$

with additional condition $\langle \sigma \rangle^{\alpha 2} = -\langle \sigma \rangle^{\alpha 4}$. We can see that sign of coupling can change depending on the sign of the $\langle u \rangle^{\alpha}$ variable ensuring proper ordering in the squared phase. More detailed analysis of the order parameter $\langle s \rangle^{\alpha} - \langle s \rangle^{\alpha 2}$ dependence on $\Delta\mu$ shows that the system should behave like ferromagnet, hence the first order transition is expected at low temperatures.

VI. SUMMARY

We have analyzed a single adlayer of oxygen atoms on W (110) surface. In the first part of our work we have presented results of a quantum mechanical DFT-cluster calculations for single oxygen atom adsorbed at W(110) surface. We evaluated the energy as a function of adatom position at its energetically optimal distance from the tungsten surface. We have found that adsorption site is shifted by about 0.45 Å from the center of rhombus formed by W atoms. That means that there are two equivalent, energetically degenerated adatom positions, separated by barrier of about 0.2 eV. This barrier is small compared with the minimal energy difference $\Delta E = 0.5$ eV that particle has to overcome when it jumps to the next adsorption site. Our calculations confirmed two-well structure of adsorption site, and large difference between energy barriers for jumps inside and out of the site. These results are in good agreement with the LEED measurements of Ynzunza *et al.*[29] and the temperature dependence of PS (Ref. 29) and the O diffusion on W(110) surface.[5–7]

Two-well structure of oxygen adsorption site is the basis for, experimentally observed,[15,16] multidomain pattern of ordered phases. We assumed that the third relatively small barrier between two minima inside single site can be easily removed by interactions with neighboring atoms. Thus in some specific configurations of neighbors, the energy minimum can be shifted. On the basis of such a scenario we have constructed three-state lattice gas model for O/W(110) systems. We have shown that our new model describes all observed phases, and does it for relatively small number of parameters. No three-particle interactions are assumed or needed. In addition to the usual phase diagram studies, our model permits one to study ordered structures with higher degeneracy of existing domains. We have shown examples for one specific choice of interacting constants. We observe that topography of the phase diagram is quite stable under change of the relative strength of interaction constants. The more detailed analysis of transition temperatures both along mean field and Monte Carlo analysis as in Ref. 12, and detailed comparison with LEED data[19–23] should establish more precisely the model parameters. Simplicity of interaction constants set allows one to analyze dynamics of the system, assuming additional barrier for jump at the saddle point that completely changes diffusion vs density relation.[42] More detailed analysis of diffusion properties of the model is under study now.

ACKNOWLEDGMENTS

This work was supported in part by KBN Grant No. 2 P03B 025 17. We acknowledge access to the computing facilities of the Interdisciplinary Center of Modelling (ICM) at Warsaw University.

[1] *Proceedings of a NATO Advanced Study Institute*: ''Surface Diffusion, Atomistic and Collective Processes,'' edited by M. C. Tringides (Plenum, New York, 1997).
[2] E. Bauer, in *Structure and Dynamics of Surfaces II*, edited by W. Schommers and P. von Blackenhagen (Springer-Verlag, Berlin, 1987).
[3] R. Gomer, Rep. Prog. Sci. **53**, 917 (1990).
[4] A. Zangwill, *Physics at Surfaces* (Cambridge University Press, Cambridge, 1988).
[5] C. Uebing and R. Gomer, Surf. Sci. **381**, 33 (1997).
[6] J. R. Chen and R. Gomer, Surf. Sci. **79**, 413 (1979).
[7] J. R. Chen and R. Gomer, Surf. Sci. **105**, 48 (1981).
[8] E. D. Williams, S. L. Cunningham, and W. H. Weinberg, J. Chem. Phys. **68**, 4688 (1978).
[9] T. Engel, H. Niehus, and E. Bauer, Surf. Sci. **52**, 237 (1975).
[10] I. Vattulainen, J. Merikoski, T. Ala-Nissila, and S. C. Ying, Phys. Rev. B **57**, 1896 (1998).
[11] W. Y. Ching, D. L. Huber, M. G. Lagally, and G. C. Wang, Surf. Sci. **77**, 550 (1978).
[12] P. A. Rikvold, K. Kaski, J. D. Gunton, and M. C. Yalabik, Phys. Rev. B **29**, 6285 (1984).
[13] D. Sahn, S. C. Ying, and J. M. Kosterlitz, in *The Structure of Surfaces II*, edited by J. F. van der Veen and M. A. van Hove (Springer-Verlag, Berlin, 1988), p. 410.
[14] M. C. Tringides, Phys. Rev. Lett. **65**, 1372 (1990).
[15] P. K. Wu, M. C. Tringides, and M. G. Lagally, Phys. Rev. B **39**, 7595 (1989).
[16] K. E. Johnson, R. J. Wilson, and S. Chiang, Phys. Rev. Lett. **71**, 1055 (1993).
[17] M. C. Tringides and R. Gomer, Surf. Sci. **155**, 254 (1985).
[18] M. C. Tringides and R. Gomer, Surf. Sci. **145**, 121 (1984).
[19] G. Ertl and D. Schillinger, J. Chem. Phys. **66**, 2569 (1977).
[20] T.-M. Lu, G. C. Wang, and M. G. Lagally, Phys. Rev. Lett. **39**, 411 (1977).
[21] M. G. Lagally, T.-M. Lu, and G. C. Wang, in *Ordering in Two Dimensions*, edited by S. Sinha (Elsevier, New York, 1980).
[22] G. C. Wang, T.-M. Lu, and M. G. Lagally, J. Chem. Phys. **69**, 479 (1978).
[23] D. H. Baek, J. W. Chung, and W. K. Han, Phys. Rev. B **47**, 8461 (1993).
[24] G. Abramovici, M. C. Desjonqures, and D. Spanjaard, J. Phys. (France) **5**, 907 (1995).
[25] A. T. Loburets, A. G. Naumovets, and Yu. S. Vedula, Surf. Sci. **399**, 297 (1998).
[26] A. G. Naumovets, M. V. Paily, and Yu S. Vedula, Phys. Rev. Lett. **71**, 105 (1993).
[27] M. A. Załuska-Kotur, S. Krukowski, and Ł. A. Turski, Surf. Sci. **441**, 320 (1999).
[28] M. A. Załuska-Kotur, S. Krukowski, Z. Romanowski, and Ł. A. Turski, Surf. Sci. **457**, 357 (2000).
[29] R. X. Ynzunza, R. Danecke, F. J. Palomares, J. Morais, E. D. Tober, Z. Wang, F. J. Garcia de Abajo, J. Liesegang, Z. Hussein, M. A. Van Hove, and C. S. Fadley, Surf. Sci. **459**, 69 (2000).
[30] D. M. Riffe and G. K. Wertheim, Surf. Sci. **399**, 248 (1998).
[31] R. J. Baxter, *Exactly Solved Models in Statistical Mechanics* (Academic, London, 1982).
[32] G. te Velde and E. J. Baerends, Chem. Phys. **177**, 399 (1993).
[33] E. Penev, P. Kratzer, and M. Scheffler, J. Chem. Phys. **110**, 3986 (1999).
[34] Z. Romanowski, S. Krukowski, I. Grzegory, and S. Porowski, J. Chem. Phys. **114**, 6353 (2001).
[35] Z. Romanowski, S. Krukowski, I. Grzegory, and S. Porowski, J. Phys.: Condens. Matter **13**, 1 (2001).
[36] P. Hohenberg and W. Kohn, Phys. Rev. **136**, 864 (1964).
[37] W. Kohn and L. J. Sham, Phys. Rev. **140**, 1133 (1965).
[38] B. Delley J. Chem. Phys. **92**, 508 (1990).
[39] A. D. Becke, Phys. Rev. **38**, 3098 (1988).
[40] C. Lee, W. Yang, and R. Parr, Phys. Rev. B **37**, 785 (1988).
[41] J. Kjoll, T. Ala-Nissila, and S. C. Ying, Surf. Sci. **218**, L476 (1989).
[42] M. A. Załuska-Kotur, S. Krukowski, and Ł. A. Turski (unpublished).